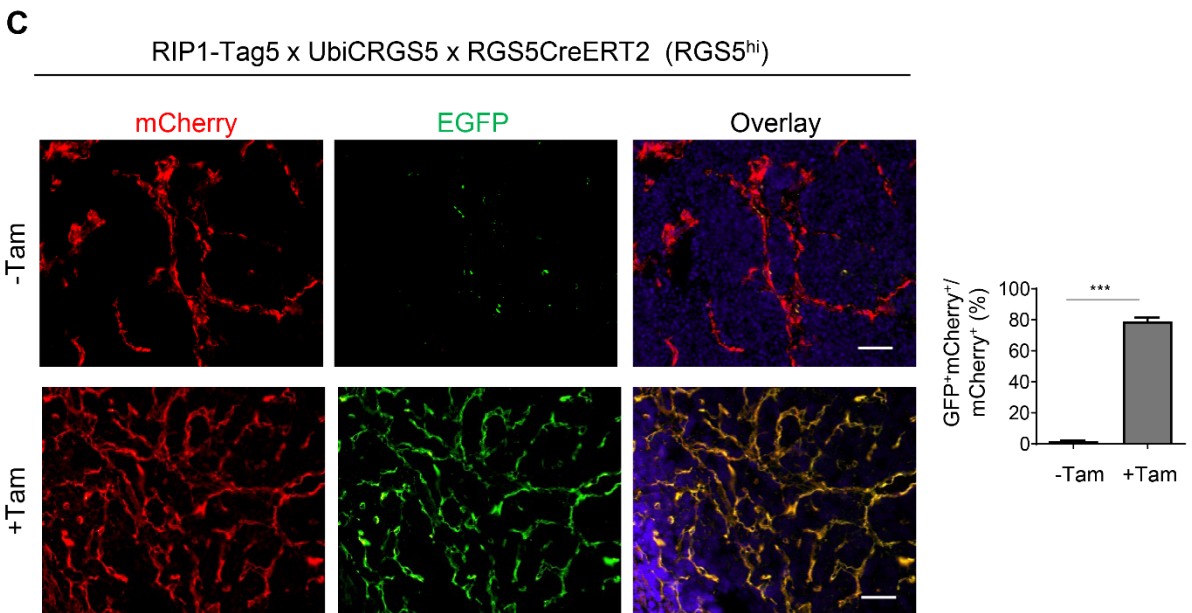
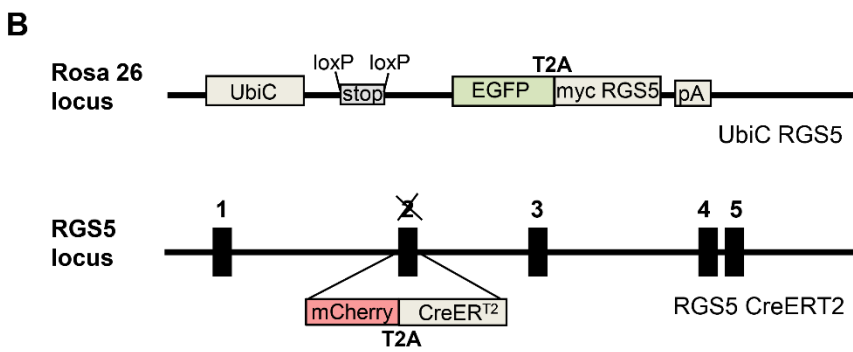
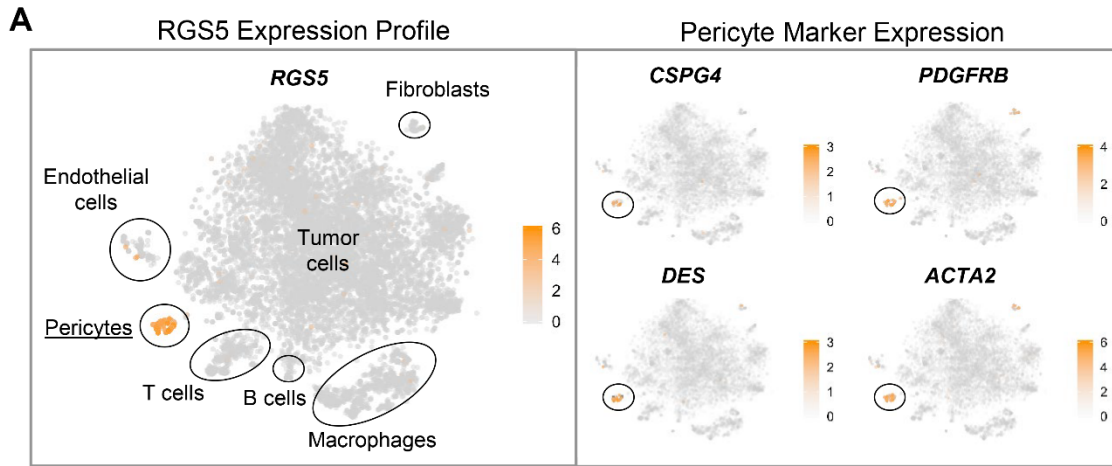


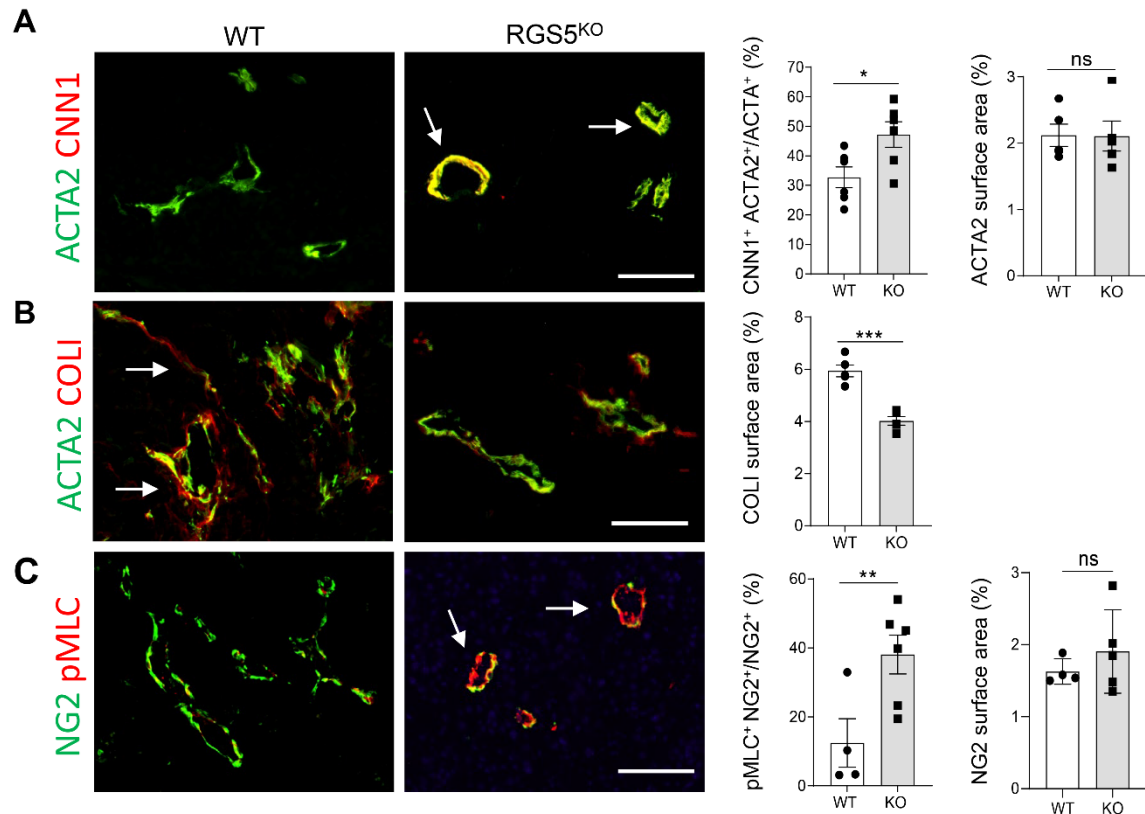
Supplemental Information

Pericyte Phenotype Switching Alleviates Immunosuppression and Sensitizes Vascularized Tumors to Immunotherapy in Preclinical Models

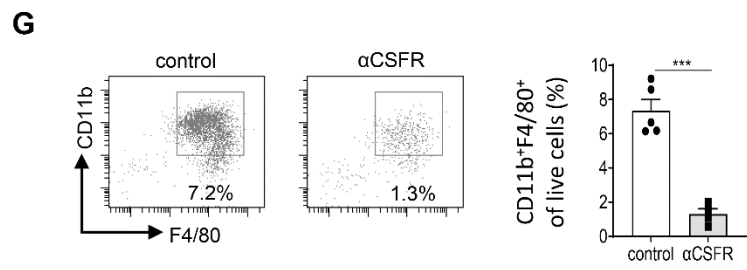
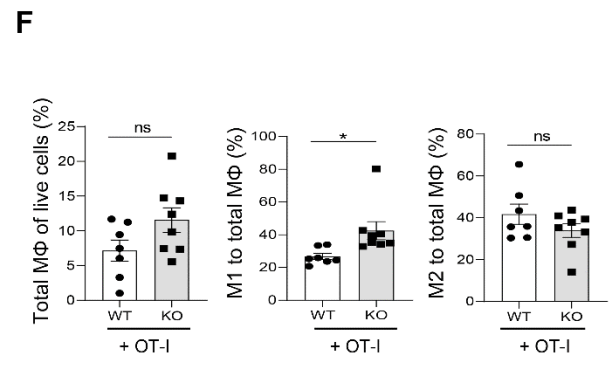
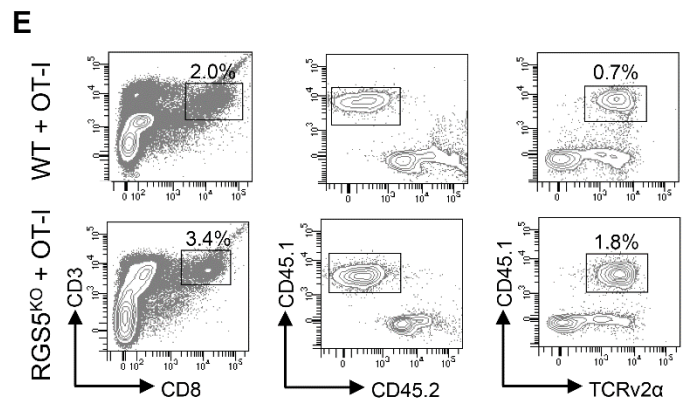
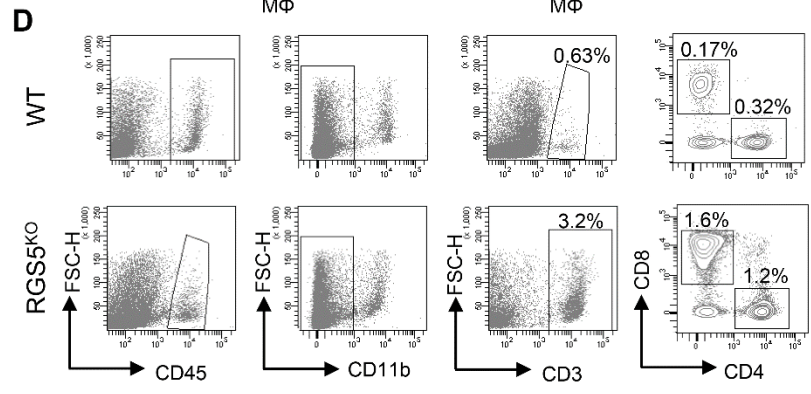
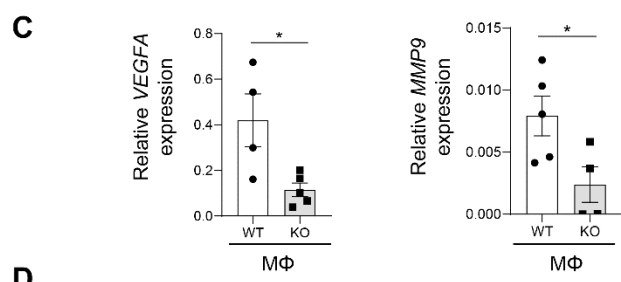
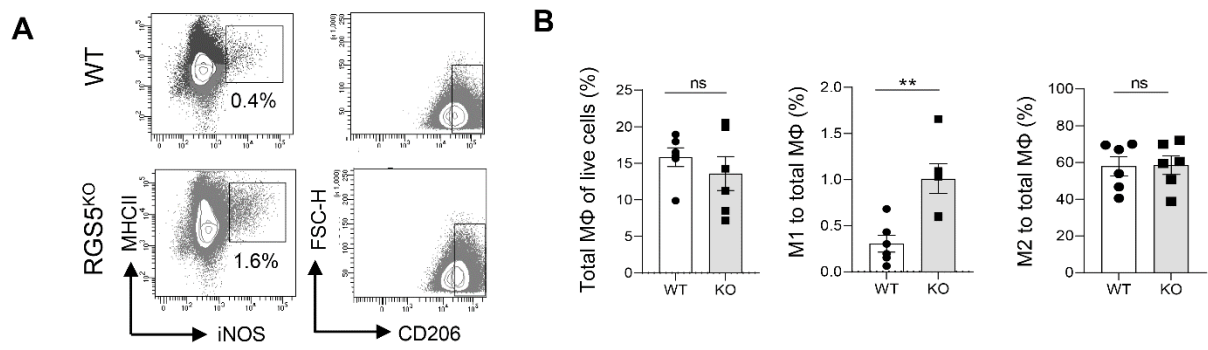
Li et al.



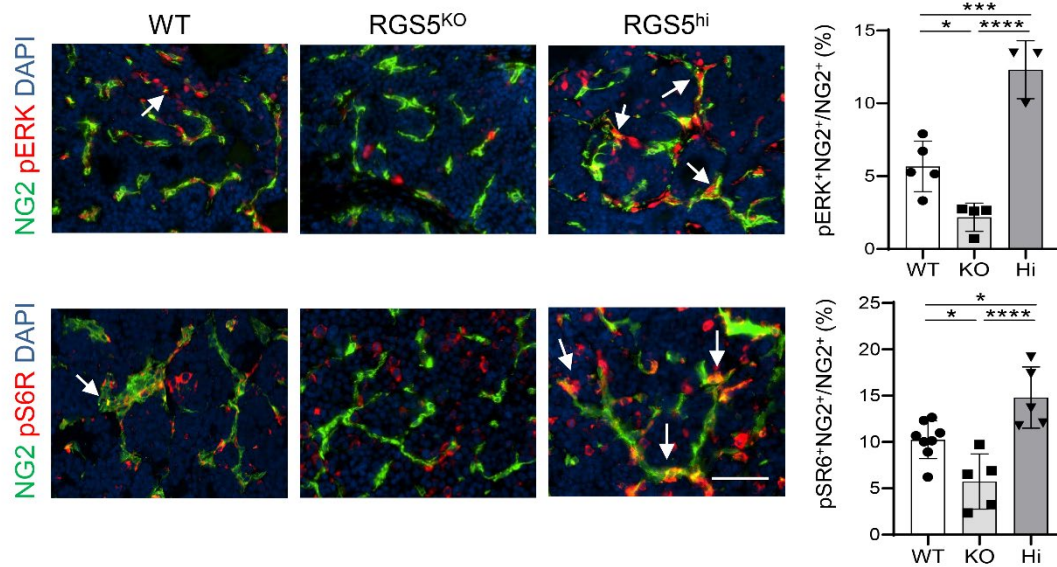
Supplemental Figure 1. RGS5 expression in PNET tumors is highly specific for pericytes and further upregulated in gain-of-function triple transgenic PNET. (A) tSNE blots of single cell RNA sequencing data from RIP1-Tag5 wild type PNET tumors. Gene clustering locates *RGS5* mRNA expression to the pericyte cluster (orange, as defined by *CSPG4* (NG2), *PDGFRB*, desmin (*DES*) and α SMA (*ACTA2*) expression), but not tumor cells, endothelial cells, fibroblasts, immune cells or monocytes/macrophages, n=3 mice. (B) Schematic diagram of two knock-in mouse lines. Upper: insertion of the UbiC promoter, *EGFP* and myc-tagged *Rgs5* genes (separated by T2A peptide) into the Rosa26 mouse locus. Expression of transgenes is prevented by a loxP flanked stop cassette. Lower: *mCherry* and *CreERT2* genes (separated by T2A) were inserted into exon 2 of the mouse *Rgs5* gene. *RGS5* overexpressing mice were generated by intercrossing the EGFP reporter line (UbiCRGS5) with the RGS5-Cre mCherry reporter mouse line (RGS5CreERT2). Further intercrossing of these 2 lines with RIP1-Tag5 (RIP1-Tag5 x UbiCRGS5 x RGS5CreERT2) generates triple transgenic, tumor-bearing mice which inherently express mCherry, and *EGFP/RGS5* driven by the endogenous *Rgs5* gene promoter upon tamoxifen induction (*Rgs5*^{hi}). (C) Representative histology of tumors in 27-week-old triple transgenic RIP1-Tag5 x UbiCRGS5 x RGS5CreERT2 mice before (-Tam, upper) and after tamoxifen (+ Tam, lower) injection at 24 weeks of age. Vascular expression of mCherry (red) and induction of vascular expression of EGFP (green) with tamoxifen are depicted. Quantification of GFP⁺ mCherry⁺ (yellow) vessels in relation to mCherry⁺ vessels (red) approximates Cre recombination rate following tamoxifen induction, n=3 mice, mean \pm SEM, ***P<0.0001. Student's t-test. Scale bars, 50 μ m.



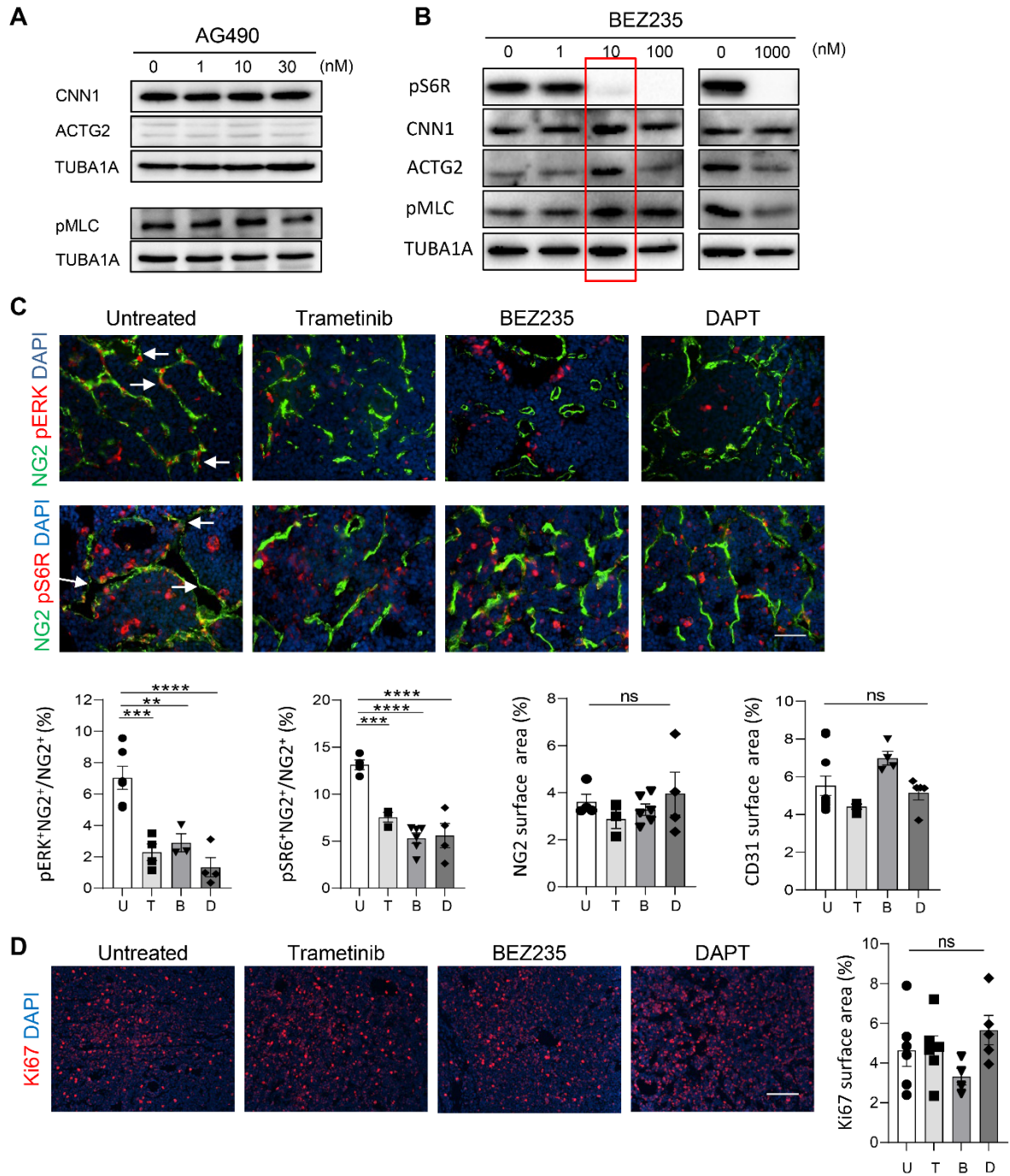
Supplemental Figure 2. B16-OVA melanoma grown in *Rgs5*^{KO} mice display an enhanced pericyte maturation status. (A) B16-OVA tumors were grown in wild type (WT) or *Rgs5* knockout (*Rgs5*^{KO} or KO) mice and CNN1 (red) coverage of ACTA2⁺ pericytes (green) was quantified (overlay yellow), n=4-6 mice, *P=0.03, ns, not statistically significant, Students's *t*-test. Scale bar, 100 μ m. (B) COLI (red) deposition around pericytes (ACTA2, green), n=4-6 mice, ***P=0.0001. Students's *t*-test. Scale bar, 100 μ m. (C) pMLC (red) expression in pericytes (NG2, green), n=4-6 mice, **P=0.02, ns, not statistically significant, Students's *t*-test. Scale bar, 100 μ m.



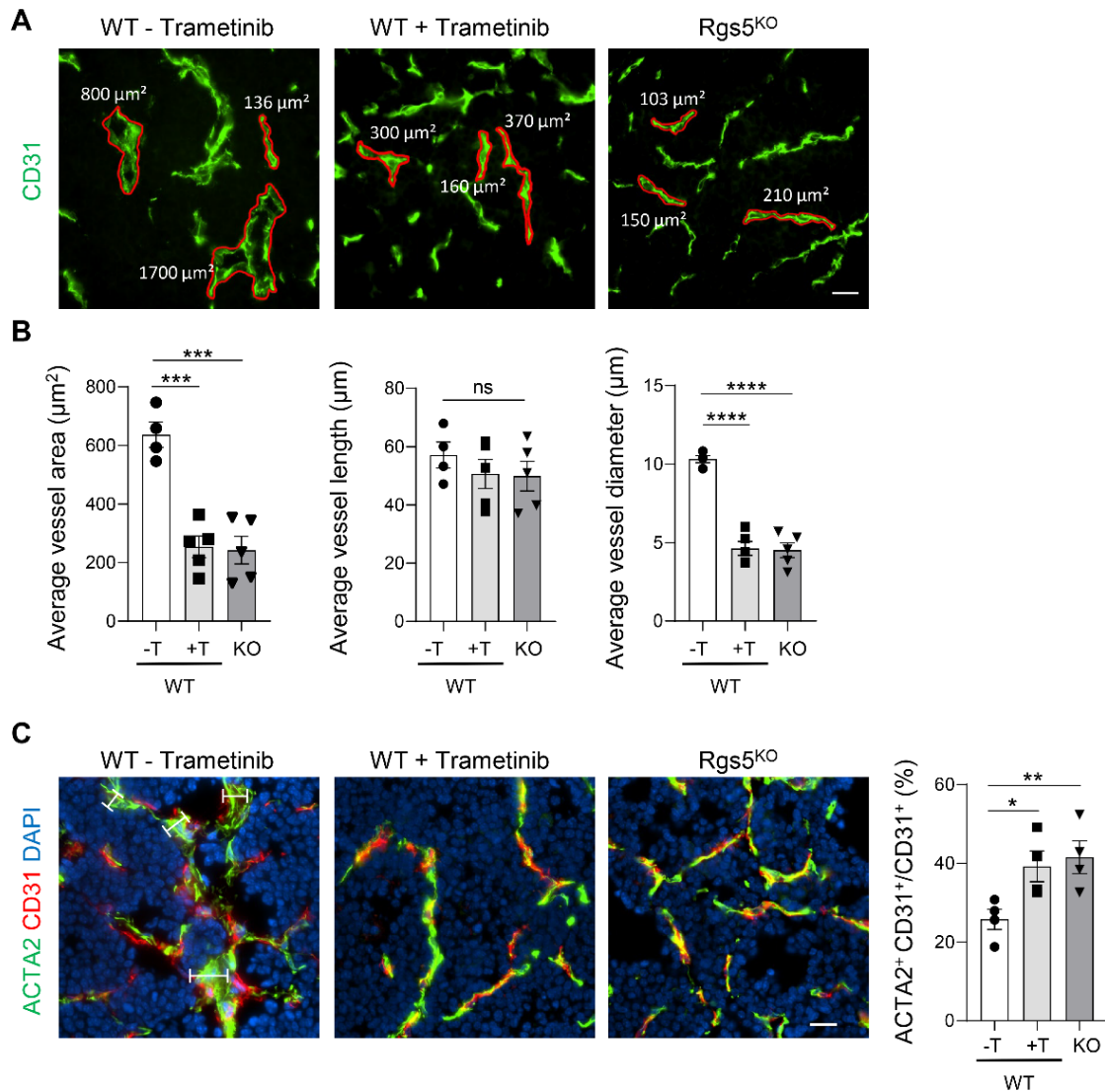
Supplemental Figure 3. Intratumoral immune cells in WT and *Rgs5*^{KO} B16-OVA tumors change in numbers and characteristics. (A) Representative FACS plots showing gating strategy for macrophage polarization in B16-OVA tumors from WT and *Rgs5*^{KO} (KO) mice. Macrophages are characterized as CD45⁺, Gr1⁻, F4/80⁺, CD11b⁺, MHCII^{high} (M1), iNOS⁺ (M1) or CD206^{high} (M2). (B) FACS quantification of total intratumoral macrophages (MΦ) gated on live cells, and percentage of M1 or M2 macrophages of total intratumoral macrophage populations in WT and *Rgs5*^{KO} B16-OVA tumors, n=4-6 mice, mean ± SEM, **P=0.003, ns, not statistically significant, Student's *t*-test. (C) CD11b⁺/F4/80⁺ B16-OVA intratumoral macrophages were sorted by FACS and *VEGFA* and *MMP9* mRNA expression quantified by qPCR, n=4-5 mice, mean ± SEM, *P=0.04 (*VEGFA*), *P=0.03 (*MMP9*), Student's *t*-test. (D) Representative FACS plots showing gating strategy for intratumoral CD45⁺, CD11b⁺, CD3⁺ CD4⁺ or CD8⁺ T cells in WT and *Rgs5*^{KO} B16-OVA tumors. (E) Representative FACS plots showing gating strategy for congenic OT-I T cells, defined as CD3⁺, CD8⁺, CD45.2⁻, CD45.1⁺, TCRv2α⁺ in WT and *Rgs5*^{KO} B16-OVA tumors following OT-I T cell transfer. (F) FACS quantification of total intratumoral macrophages (MΦ) gated on live cells following adoptive OT-I transfer, and percentage of M1 or M2 macrophages of total macrophage populations following OT-I transfer, n=7-8 mice, mean ± SEM, *P=0.025, ns, not statistically significant, Student's *t*-test. (G) Representative FACS blots and quantification of CD11b⁺, F4/80⁺ intratumoral macrophages, gated on live cells, in untreated B16-OVA tumors (control), and tumors treated with macrophage-depleting αCSFR antibodies, n=4-5 mice, mean ± SEM, ***P=0.0001, Student's *t*-test.



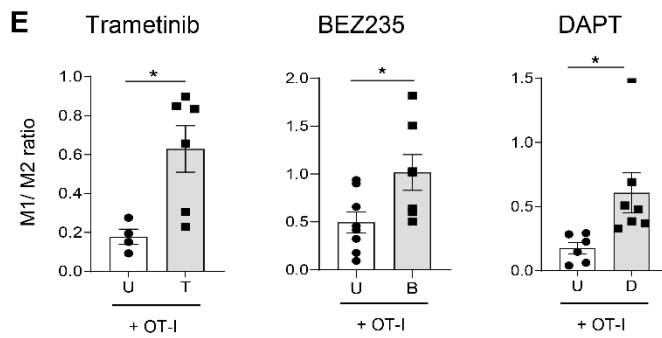
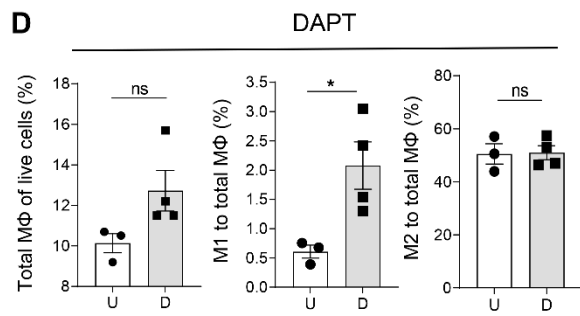
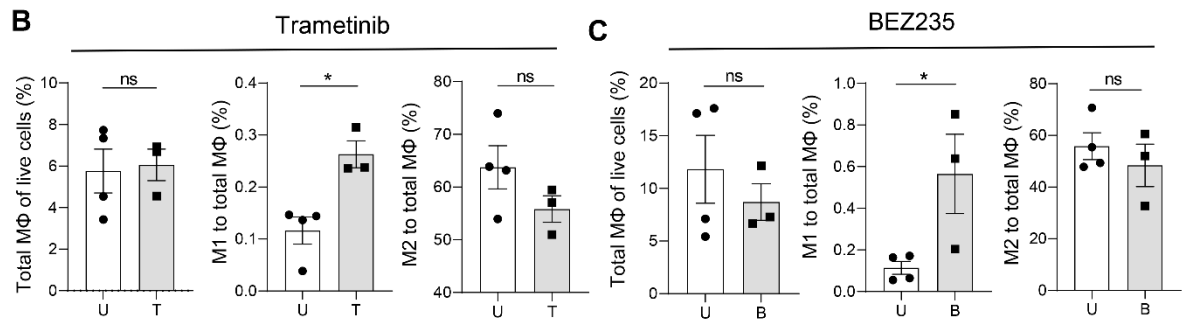
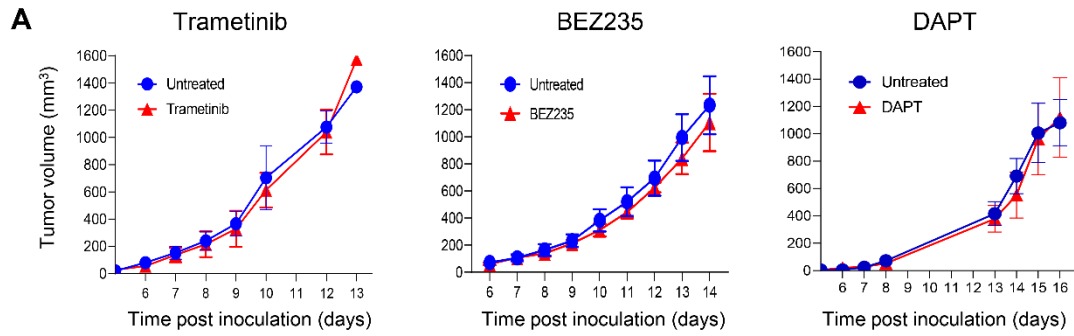
Supplemental Figure 4. pERK and pS6R vascular expression correlates with RGS5 levels in PNET tumors. Representative images from 27-week-old RIP1-Tag5 tumors grown in WT, *Rgs5*^{KO} (KO), or *Rgs5*^{hi} (Hi) mice depicting MEK/ERK signaling (pERK, red, upper) in NG2⁺ pericytes (green), or AKT signaling (pS6R, red, lower) in NG2⁺ pericytes (green), arrows indicate overlay (yellow). Quantification of vascular signaling: pERK, n=3-5 mice, mean ± SEM, *P=0.024, ***P=0.0008, ****P=<0.0001, one-way ANOVA. pS6R, n=5-8 mice, *P<0.026, ****P=0.002, one-way ANOVA. Scale bar, 50 μm.



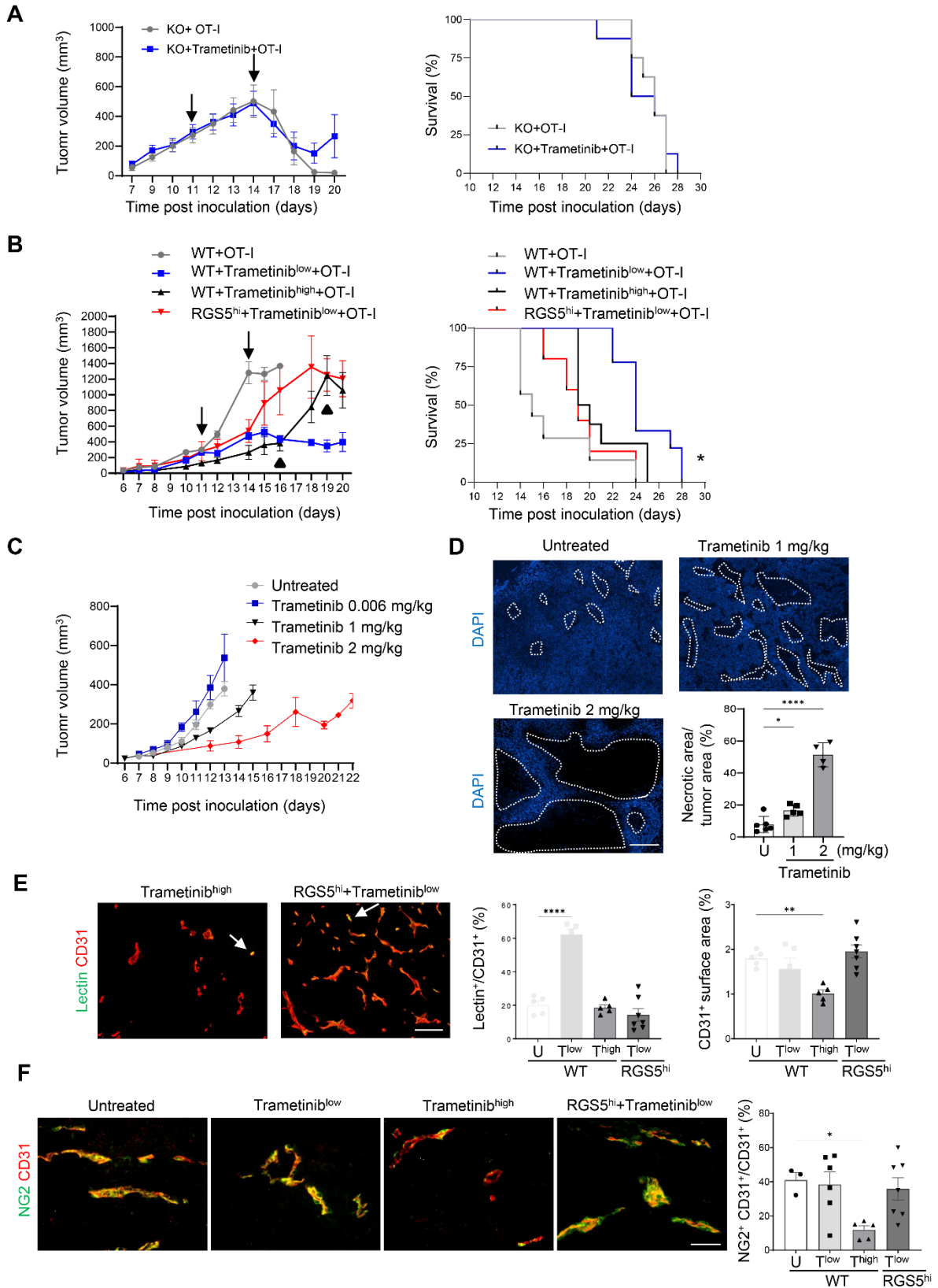
Supplemental Figure 5. Contractile marker induction in vitro is dose dependent and pERK and pS6R vascular expression is reduced after low dose drug treatment. (A) WB of contractile pericyte markers (CNN1, ACTG2) in correlation to Rho kinase activity (pMLC) in 10T1/2 RGS5myc cells following a 24 h incubation with increasing doses of AG490. The experiment was conducted twice. (B) Representative WB of AKT signaling (pS6R), contractile pericyte markers (CNN1, ACTG2) in correlation to Rho kinase activity (pMLC) in RGS5myc cells following a 24 h incubation with increasing doses of the PI3K inhibitor BEZ235. The experiment was conducted twice. (C) Representative images from untreated (U) RIP1-Tag5 mice, or following treatment from week 27 to 29 with trametinib (T, 0.02 mg/kg), BEZ235 (10 mg/kg), or DAPT (10 mg/kg) assessing vascular pERK (red, upper) or pS6R (red, lower) expression in pericytes (NG2, green). Arrows indicate overlay (yellow). Quantification of vascular signaling: pERK, **P=0.0053, ***P=0.0008, ****P=0.0001; pS6R: ***P=0.0015, ****P<0.0001; NG2⁺ pericytes and CD31⁺ blood vessels: ns, not statistically significant, n=3-6 mice, mean ± SEM, one-way ANOVA. Scale bar, 50 μm. (D) Tumor cell proliferation index following drug treatment in RIP1-Tag5 mice as assessed by Ki67 staining and quantification, n=4-6 mice, ns, not statistically significant, mean ± SEM, one-way ANOVA. Scale bar, 100 μm.



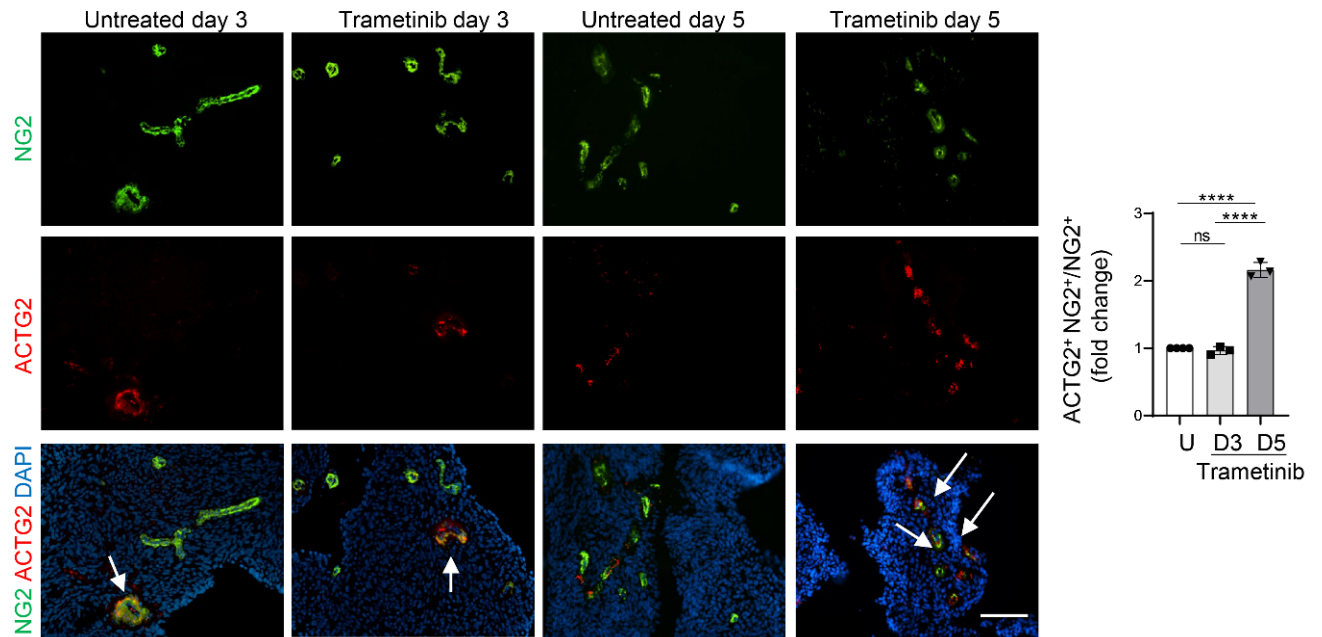
Supplemental Figure 6. *Rgs5* gene knockout or trametinib treatment stabilize PNET tumor vessels. (A) Untreated PNET-bearing RIP1-Tag5 mice (WT - T) or WT mice treated with trametinib for 2 weeks (WT + T), or *Rgs5*^{KO} (KO) mice, were stained for CD31⁺ tumor vessels (green) and average tumor vessel area demarcated in red. Scale bar, 20 μm . (B) Quantification of tumor vessel area (left), tumor vessel length (middle) and calculation of tumor diameters (right), $n=4-5$ mice, mean \pm SEM, *** $P=0.00001$, **** $P<0.00001$, ns, not statistically significant, one-way ANOVA. (C) Same groups as in (A) were analyzed for ACTA2⁺ (green) pericyte alignment with CD31⁺ (red) endothelial cells and ACTC2⁺ covered CD31⁺ blood vessels quantified (yellow). Brackets indicate broad/fuzzy appearance of pericytes protrusions into parenchyma, $n=4$ mice, mean \pm SEM, * $P=0.0488$, ** $P=0.0236$, one-way ANOVA. Scale bar, 20 μm .



Supplemental Figure 7. Low dose drug treatment changes macrophage phenotypes but does not reduce tumor growth. (A) Wild type mice bearing B16-OVA tumors were left untreated or treated from day 6 with 10 oral doses of trametinib (0.006 mg/kg, n=3-4 mice), BEZ235 (10 mg/kg, n=6-7 mice), or DAPT (10 mg/kg, n=6 mice), and tumor growth was monitored. (B) B16-OVA trametinib treatment: quantification of total intratumoral macrophages, gated on live cells, and percentage of M1 (MHCII^{hi}, iNOS⁺) or M2 (CD206^{high}) macrophages in total intratumoral macrophage populations, n=3-4 mice, mean ± SEM, *P=0.0115, ns, statistically not significant, Student's *t*-test. (C) B16-OVA BEZ235 treatment: quantification of total intratumoral macrophages, gated on live cells, and percentage of M1 or M2 intratumoral macrophages in total macrophage populations, n=3-4 mice, mean ± SEM, *P=0.04, ns, statistically not significant, Student's *t*-test. (D) B16-OVA DAPT treatment: quantification of total intratumoral macrophages, gated on live cells, and percentage of M1 or M2 intratumoral macrophages in total macrophage populations, n=3-4 mice, mean ± SEM, *P=0.03, ns, statistically not significant, Student's *t*-test. (E) Intratumoral M1/M2 macrophage ratios in trametinib (left), BEZ235 (middle) or DAPT (right) treatment groups following one adaptive OT-I T cell transfer, n=3-5 mice, mean ± SEM, *P=0.02 (trametinib), *P=0.03 (BEZ235 and DAPT), Student's *t*-test.



Supplemental Figure 8. Vessel functionality is critical for the success of low dose drug combination immunotherapy. (A) *Rgs5*^{KO} (KO) B16-OVA mice were treated with adoptive OT-I T cell transfers (arrows) with or without trametinib (0.006 mg/kg). Tumor growth and survival of n=8 mice, mean ± SEM. (B) WT or RGS5 overexpressing (*Rgs5*^{hi}) B16-OVA tumors received no drug or were treated with trametinib at different doses (Trametinib^{low}: 0.006 mg/kg; Trametinib^{high}: 1 mg/kg), followed by adoptive transfers of OT-I cells when tumor volume reached 300-400 mm³ (indicated by arrows for all groups with the exception of WT/Trametinib^{high} where arrow heads indicate delayed transfers). Tumor growth (n=5-10) and survival of n=5-9 mice, mean ± SEM. Survival was terminated on day 30, *P=0.001, WT Trametinib^{low} versus WT no Trametinib; *P=0.02, WT Trametinib^{low} versus WT Trametinib^{high}; *P=0.005, WT Trametinib^{low} versus *Rgs5*^{hi} Trametinib^{low}, log rank (Mantel-Cox) test. (C) Assessment of tumor growth kinetics in untreated compared to WT B16-OVA mice treated with increasing doses of trametinib, n=3-10 mice, mean ± SEM. (D) DAPI nuclear stain and quantification of B16-OVA tumor necrosis defined as absence of nuclear stain (dotted lines) following trametinib treatment, n=4-6, mean ± SEM, *P=0.035, ****P<0.0001, one-way ANOVA. Scale bar, 500 μm. (E) Assessment of tumor perfusion following trametinib treatments. CD31 (red) overlay with infused FITC-lectin (yellow) is highlighted by arrows. Perfusion and vessel numbers were quantified in WT B16-OVA mice treated with 1 mg/kg trametinib (T^{high}), or *Rgs5*^{hi} B16-OVA mice treated with low dose trametinib (*RGS5*^{hi} + T^{low}) in comparison to untreated and 0.006 mg/kg (T^{low}) treatment groups (data from Figure 5A, shadowed), n=5-7 mice, mean ± SEM, **P=0.0083, ****P<0.0001, one-way ANOVA. Scale bar, 100 μm. (F) Pericyte (NG2⁺, green) vessel (CD31⁺, red) coverage in B16-OVA treatment groups, n=3-7, *P=0.034, one-way ANOVA. Scale bar, 50 μm.



Supplemental Figure 9. Trametinib induces the contractile marker ACTG2 in brain cancer pericytes. Microscopic images of meningioma tumor slices cultured ex vivo for 3 or 5 days with or without trametinib. ACTG2 staining (red) depicts mature ACTG2⁺ covered (yellow, arrows) NG2⁺ (green) pericytes. Quantification of ACTG2 covered NG2⁺ pericytes in untreated meningioma slices (U, day 3, day 5), and slices incubated with 50 mM trametinib for 3 and 5 days (D3, D5), n=3 patients, mean \pm SEM, ****P<0.0001, ns, not statistically significant, one-way ANOVA. Scale bar, 100 μ m.

Table 1. Antibodies for Western Blot and Immunohistochemistry

Name	Host	Clone	Color	Catalogue #	Source	Antibody ID
Western blot						
ACTG2	rabbit	polyclonal	-	NB100-91649	Novus	AB_1216156
AKT (pan)	rabbit	monoclonal	-	4691	Cell Signaling	AB_915783
pAKT (Ser 473)	rabbit	D93	-	4060	Cell Signaling	AB_2315049
CNN1	rabbit	EP798Y	-	46794	Abcam	AB_2291941
CNX43	rabbit	polyclonal	-	C6290	Sigma	AB_476857
ERK1/2 (pan)	rabbit	137F5	-	4695	Cell Signaling	AB_390779
pERK (Thr202/Tyr204)	rabbit	D13.14.4E	-	4376	Cell Signaling	AB_2315112
Foxo3a (pan)	rabbit	75D8	-	2497	Cell Signaling	AB_836876
pFoxo3a (Thr32/Thr24)	rabbit	polyclonal	-	9464S	Cell Signaling	AB_329842
KLF4 (H-180)	rabbit	polyclonal	-	sc20691	Santa Cruz	AB_669567
pMLC (Ser20)	rabbit	polyclonal	-	ab2480	Abcam	AB_303094
P27KIP1 (pan)	rabbit	polyclonal	-	sc3674	Santa Cruz	AB_632129
pP27KIP1 (Thr187)	rabbit	polyclonal	-	sc16324-R	Santa Cruz	AB_670358
ROCK 1	rabbit	polyclonal	-	4035s	Cell Signaling	AB_2238679
ROCK2	rabbit	polyclonal	-	8236s	Cell Signaling	AB_10829468
ACTA2	mouse	14A	FITC	F3777	Sigma	AB_476977
TUBA1A	mouse	B-5-1-2	-	T6074	Sigma	AB_477582
Immunohistochemistry						
ACTG2	rabbit	polyclonal	-	AP06002PU	OriGene	AB_1610944
CD3e	rabbit	polyclonal	-	52959	Abcam	AB_868901
CD31	rat	MEC13.3	-	550274	BD Biosciences	AB_393571
CD31	rat	SZ31	-	DIA-310	Biozol	AB_2631039
CD31- biotin	rat	MEC13.3	-	553371	BD Biosciences	AB_394817
CDH5 (CD144)	rat	11D4.1	-	555289	BD Biosciences	AB_395707
CNN1	rabbit	EP7998Y	-	ab46794	Abcam	AB_2291941
CALD1	rabbit	E89	-	ab32330	Abcam	AB_725810
CNX43	rabbit	polyclonal	-	C6290	Sigma	AB_476857
COL1	rabbit	polyclonal	-	PAB13488	Abnova	AB_10556808
EGFP	rabbit	polyclonal	-	GTX113617	GeneTex	AB_1950371
pERK	rabbit	D13.14.4E	-	4370S	Cell Signaling	AB_2315112
Ki67	rat	SoIA15	-	14-5698-82	Thermo Fisher	AB_10854564
mCherry	mouse	1C51	-	ab125096	Abcam	AB_11133266
pMLC (Ser20)	rabbit	polyclonal	-	ab2480	Abcam	AB_303094
NG2	rabbit	polyclonal	-	AB5320	Millipore	AB_91789
NG2	rat	1E6.4	-	130-097-455	Miltenyi Biotec	AB_2651235
SMA, alpha	mouse	1A4	FITC	3777	Sigma	AB_476977
pS6Rp	rabbit	D57.2.2E	-	4858S	Cell Signaling	AB_916156
ICAM	hamster	3E2B	-	MA5405	Invitrogen	AB_223595

Table 2. Antibodies for FACS and Secondary Antibodies

Name	Host	Clone	Color	Catalogue #	Source	Antibody ID
FACS						
CD3e	hamster	eBio500A2	PerCp-eFlour 710	46-0033-82	Thermo Fisher	AB_10597122
CD3e	hamster	145-2C11	FITC	553062	BD Biosciences	AB_394595
CD4	rat	Gk1.5	BUV737-APC	100412	BioLegend	AB_312697
CD8	rat	53-6-7	PE	553033	BD Biosciences	AB_394571
CD11b	rat	M1/70	APC-Cy7	101226	BioLegend	AB_830642
CD45	rat	30F-11	PE-CF594	562420	BD Biosciences	AB_11154401
CD45.1	mouse	A20	BUV737	564574	BD Biosciences	AB_2738850
CD45.2	mouse	104	PE-Cy7	560696	BD Biosciences	AB_1727494
CD206	rat	C068C2	PE-Cy7	141720	BioLegend	AB_2562248
F4/80	rat	BM8	APC	123116	BioLegend	AB_893481
Gr-1	rat	RB6-8C5	PE	108408	BioLegend	AB_313373
iNOS	rat	CXNFT	AF-488	53-5920-82	Thermo Fisher	AB_2574423
MHCclass II (I-A/I-E)	rat	M5/114.15.2	PerCP-Cy5.5	107626	BioLegend	AB_2191071
TCRv2α	rat	B20.1	APC	127810	BioLegend	AB_1089250
Secondary Antibodies						
anti-FITC	goat	polyclonal	biotin	ab6655	Abcam	AB_305628
anti-goat IgG	donkey	polyclonal	AF488	ab150129	Abcam	AB_2687506
anti-hamster IgG	goat	polyclonal	AF488	A21110	Thermo Fisher	AB_2535759
anti-hamster IgG	rabbit	polyclonal	Cy3	307165003	Jackson	AB_2339586
anti-mouse IgG	goat	polyclonal	Dylight 405	115475003	Jackson	AB_2338786
anti-mouse IgG	horse	polyclonal	HRP	PI-2000	Vector	AB_2336177
anti-rabbit IgG	donkey	polyclonal	AF488	A21206	Thermo Fisher	AB_243579
anti-rabbit IgG	donkey	polyclonal	AF594	A21207	Thermo Fisher	AB_141637
anti-rabbit IgG	goat	polyclonal	HRP	PI-1000	Vector	AB_1000
anti-rat IgG AF488	donkey	polyclonal	AF488	A21208	Thermo Fisher	AB_2535794
anti-rat IgG	donkey	polyclonal	AF459	A21209	Thermo Fisher	AB_2435795
Anti-rat IgG	donkey	polyclonal	Dylight 405	712-475-153	Jackson	AB_2340681